Picosecond Time-Resolved Transient Grating Method for Heat Detection: Excited-State Dynamics of $FeCl_3$ and *o*-Hydroxybenzophenone in Aqueous Solution

Toshiya Okazaki, Noboru Hirota, and Masahide Terazima*

Department of Chemistry, Graduate School of Science, Kyoto University, Kyoto 606, Japan

Received: July 8, 1996; In Final Form: October 4, 1996[⊗]

Transient grating signals after photoexcitation to electronically excited states of $FeCl_3$ and *o*-hydroxybenzophenone (*o*-HBP) in aqueous solutions were investigated at various temperatures with short-pulsed laser systems. The observed signals can be expressed by a superposition of the density grating (Dens.G) signal and the temperature grating (Temp.G) signal. Above 4 °C, an acoustic oscillation is predominant in the signal, while the acoustic oscillation disappears and a pure Temp.G signal is observed clearly at 4 °C. The rise profile of the pure Temp.G signal was analyzed in terms of the deactivation from the photoexcited state, and it is found that a very fast thermalization process takes place among the solvent molecules. The lifetime of the charge-transfer state of $[Fe(OH)(H_2O)_5]^{2+}$ is determined to be 55 ps from the rise profile of the Temp.G signal. Using a subpicosecond laser system and the population grating signal, two time constants (400 fs and 7.5 ps) are obtained for the dynamics of *o*-HBP. The dynamics of the photoexcited states of $FeCl_3$ and *o*-HBP are also discussed. Since the temporal response of the Temp.G component is 10−100 times shorter than that of the Dens.G signal, this signal can be used for studying ultrafast heat-releasing processes.

1. Introduction

Photoexcited molecules relax to their original ground states radiatively or nonradiatively if chemical reactions do not occur. In the condensed phase, radiationless processes such as vibrational relaxation, internal conversion, and intersystem crossing are generally much more dominant than radiative processes. Therefore, detection of radiationless transitions is important for elucidating the photophysical properties of molecules.

The transient grating (TG) method is well-known to be highly sensitive to detect the radiationless transition of the thermal energy with fairly fast time resolution as discussed below.[1−8] The TG signal appears whenever the variation of the refractive index of the system is induced. The variation of the refractive index of the solvent (Δn) after the thermal energy is deposited into the medium can be expressed by

$$\Delta n = \left[\left(\frac{\partial n}{\partial \rho}\right)_T \left(\frac{\partial \rho}{\partial T}\right) + \left(\frac{\partial n}{\partial T}\right)_\rho\right]\Delta T \qquad (1)$$

where T is the temperature and ρ is the density of the solvent. The first term is the variation of the refractive index due to the density changes, and the second term is due to the temperature changes without density change. In many organic solvents, the first term dominates over the second term.[7,9,10] Generally, the density change does not take place immediately after the heat release, and this time constant is determined by the acoustic transit time $\tau_{ac} = \Lambda/v$ (Λ is the fringe spacing of the grating and v is the speed of sound in the medium). Therefore, the speed of the density change after heating is important for determining the time resolution of this method. Genberg et al. reported that the maximum time resolution of the TG method based on the first term of eq 1 is ∼20 ps,[3] and it may be widely recognized that, under normal experimental conditions, the time resolution for heat detection by this method is on the order of 50−100 ps.

Many energetic relaxation processes after photoexcitation of molecules occur on a time scale of around several picoseconds.[11,12] For example, the lifetime of the lowest excited singlet (S_1) state can be between 1 ps and a few nanoseconds, and the time constant of vibronic relaxation is normally in the range 1−100 ps. Therefore, these processes cannot be investigated by the usual TG method because of the low time resolution. Recently, Terazima found a new photothermal signal which originates from the second term in eq 1 by the TG and the thermal lens (TL) methods, and those are called the temperature grating (Temp.G) signal and the temperature lens (Temp.L) signal, respectively.[6,7,13−15] (The signals originating from the first term were called the density grating (Dens.G) and the density lens (Dens.L) signals.) In ref 6, he used water as the solvent for demonstrating the existence of the Temp.L and Temp.G components, because the effect of the second term on water can be relatively larger than that of the first term depending on the temperature. This Temp.G (Temp.L) signal potentially has a very fast time response since the temperature change should appear immediately after the heating. In that study, however, since he used a nanosecond pulsed laser for the excitation, the maximum time resolution was of the order of nanoseconds; i.e., this time resolution was determined by the pulse width of the excitation beam.

In this paper, we first demonstrate a picosecond time resolution of the Temp.G signal using a picosecond pulsed laser system. On the basis of these results, we applied the Temp.G method to investigate the dynamics of the photoexcited states of two chemical systems: $FeCl_3$ and *o*-hydroxybenzophenone (*o*-HBP). The photoexcited states of $FeCl_3$ in water have been investigated and sometimes used as a calorimetric reference in aqueous medium.[16] However, the photophysical dynamics have not been studied so far. The reason may be due to the fact that the transient absorption of this sample is too weak to be detected. Even for such a dark molecule, the excited-state dynamics can be investigated by the heat-detection methods such as the TG method.

The second example, *o*-HBP, is well-known as a photochemical stabilizer, and the photophysical dynamics is interesting with respect to the efficient energy dissipation mechanism.[17−19] Hou et al. studied excited-state energy relaxation in hexane (non-

[⊗] Abstract published in *Advance ACS Abstracts,* December 15, 1996.

S1089-5639(96)02018-X CCC: $14.00 © 1997 American Chemical Society

hydrogen-bonding solvent) and ethanol (hydrogen-bonding solvent) by the transient absorption method with a picosecond laser system.[17] In hexane, only a short-lived component was observed with a lifetime of ~35 ps, and they attributed this component to the lifetime of the excited singlet (S_1) state of an intramolecularly hydrogen-bonded species. On the other hand, in ethanol, short-lived (~30-ps) and long-lived (~1.5-ns) components were observed. They concluded that in this solvent, both intramolecularly and intermolecularly hydrogen-bonded *o*-HBP exist before photoexcitation, and the short-lived one was attributed to the excited singlet state of an intramolecularly hydrogen-bonded species and the long one to the lowest triplet (T_1) state of an intermolecularly hydrogen-bonded species. The short excited-state lifetime of the intramolecularly hydrogen-bonded species was explained by a highly efficient energy wasting channel caused by the hydrogen bonding. On the other hand, Merritt et al. reported ~10 ps as the lifetime of the S_1 state in methylene chloride[18] and also reported that Topp obtained 6 ps in hexane and 30 ps in ethanol.[20] The difference of these lifetimes could be due to the weak intensity of the transient absorption of *o*-HBP. In this paper, we measure the energy relaxation dynamics of *o*-HBP in a non-hydrogen-bonding solvent by the newly developed Temp.G method and also by the population grating method using a subpicosecond laser system.

2. Experimental Section

The experimental setup for the picosecond time-resolved transient grating experiment is similar to that reported previously.[8] The third harmonic of a Nd:YAG laser pulse (Continuum PY61c-10; $\lambda = 355$ nm) and a Nd:YAG laser-pumped dye laser pulse (Continuum PD10; $\lambda = 640$ nm) were used for the excitation and for probing the grating, respectively. Each pulse width was about 35 ps. The laser power of the pump beam was 2−40 μJ/pulse (depending on the temperature of the sample). The pump beam was split into two with a beam splitter. These beams were focused by lenses ($f = 25$ cm) and crossed about 30° inside the quartz sample cell in order to generate an optical interference pattern. The probe beam passed through an optical delay line was focused by a lens ($f = 20$ cm) and brought into the sample cell by an angle that satisfied the Bragg condition. The diffracted TG signal was separated from other beams with a pin hole and a glass filter (Toshiba R-60) and detected by a photomultiplier. The detected TG signal was averaged with a boxcar integrator (EG&G Model 4400 Series) and with a personal computer.

A pulse of a Nd:YAG laser (Coherent Antares 76-S)-pumped dye laser (Coherent Satori 774; $\lambda = 640$ nm), which was amplified with a dye amplifier system (Continuum PTA60 and Continuum RGA60), was used for measuring the population grating signal of *o*-HBP in the faster time scale (pulse width ~350 fs). The amplified pulse was split into three with two beam splitters. The frequency of the two beams was doubled to 320 nm by BBO crystals and used as excitation beams. The laser pulse energy was ~1 μJ. The other pulse was used as a probe beam.

The temperature of the sample solution was controlled by flowing methanol around a metal cell holder. A thermostated bath (Lauda RLS6-D) was used to circulate the methanol. The temperature of the cell holder was monitored by a thermocouple wire, and the voltage was monitored by a digital volt meter. The stability of the temperature was 0.1 °C.

The samples, iron(III) chloride (Nacalai Tesque) and *o*-hydroxybenzophenone (*o*-HBP; Tokyo Kasei), and the surfactant, sodium lauryl sulfate (SDS; Nacalai Tesque), were used without further purification. The solvent, distilled water, and hexane (Nacalai Tesque) were used as received. The sample solution was flowed so that a fresh sample solution was photoexcited continuously.

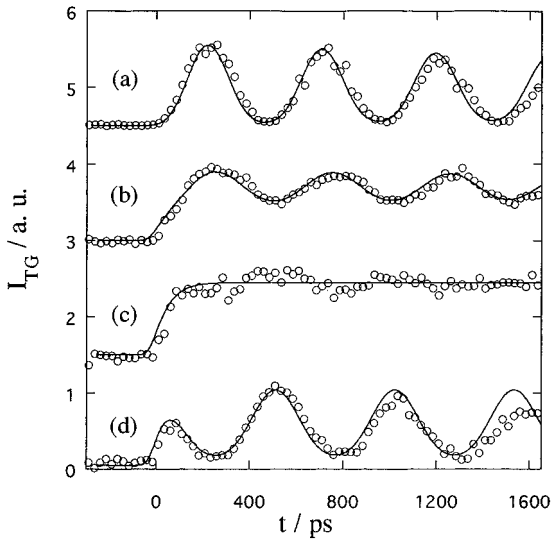

Figure 1. Time profile of the TG signals of $FeCl_3/H_2O$ (10 mM) at various temperatures: (a) 22, (b) 6, (c) 4, (d) 2 °C. The solid lines are the best-fit calculated signals with a rise time of 55 ps. The other parameters used for the calculation are listed in text.

3. Results and Discussion

3-1. Temp.G Signal in the Picosecond Time Scale. As described in the Introduction, Terazima previously showed the existence of a Temp.G component in the TG signal clearly by using the temperature variation method with the nanosecond pulsed laser system.[6] Here, first, we demonstrate a similar experiment using the picosecond pulsed laser in a fast time scale. Figure 1 shows the temporal profiles of the observed TG signal after photoexcitation of $FeCl_3/H_2O$ (10 mM) at several temperatures. At high temperatures (such as 22 °C, Figure 1a), a sinusoidal oscillation is observed. This oscillation can be explained by the acoustic signal which is produced by the spatially periodic photoexcitation of the sample and subsequent heating processes by the nonradiative transition from the excited state.

The observed oscillation is fitted by a calculation as follows. The spatially periodic excitation is achieved by the interference pattern between two excitation beams. When a probe beam is brought into the grating region at the Bragg angle, a part of the probe beam is diffracted to a phase-matching direction (TG signal). According to the coupled wave theory, the intensity of the TG signal (I_{TG}) is given by[21]

$$I_{TG} = \alpha(\Delta n)^2 + \beta(\Delta k)^2 \qquad (2)$$

where α and β are constants which are determined by the experimental conditions such as the crossing angle, the wavelength of the pump beams, the absorbance of the sample, and the grating thickness, and Δn, and Δk denote the peak−null differences in the refractive index and the absorbance, respectively. If there is no absorption of the probe beam by the solute and photoexcited species ($\Delta k \approx 0$), one of the dominant contributions comes from the change of the refractive index caused by the variation of the density (density grating (Dens.G)). We assume that the heat energy, Q, is deposited into the medium by deactivation processes from excited state i; that is,

$$Q = \sum_i 2Q_i\{1 - \exp(-\gamma_i t)\}(1 + \cos qx) \quad (3)$$

where $1/\gamma_i$ is the lifetime of excited state i, q is the magnitude of the wavevector of the grating, x denotes the coordinate to the fringes, and Q_i is the thermal energy from excited state i in unit volume. The time profiles of the Dens.G term ($\Delta n_\rho(t)$) is described by[3,8]

$$\Delta n_\rho(t) \simeq \left(\frac{\partial n}{\partial \rho}\right)_T \left\{\sum_i AQ_i(b^2 + \omega^2)^{-1} \times \left[\frac{b}{\omega}\sin(\omega t)\exp(-d_a t) - \cos(\omega t)\exp(-d_a t) + \exp(-bt)\right] - AQ_i({\gamma_i}^2 + \omega^2)^{-1} \times \left[\frac{\gamma_i}{\omega}\sin(\omega t)\exp(-d_a t) - \cos(\omega t)\exp(-d_a t) + \exp(-\gamma_i t)\right]\right\} \quad (4)$$

where $\omega = vq$ (v is the speed of sound in the solution), d_a is the acoustic attenuation rate constant, $b = \lambda_w q^2/\rho_0 C_p$ (λ_w is the thermal conductivity, C_p is the specific heat, and ρ_0 is the density of the solvent), and $A = 2q^2\alpha/\kappa\rho_0 C_p$ (α is the coefficient of thermal expansion and κ compressibility). The observed signal at 22 °C can be fitted by this equation with the parameters of $\omega = 1.29 \times 10^{10}$ s^{-1}, $q = 8.7$ μm^{-1}, $b = 5.9 \times 10^6$ s^{-1}, $v = 1480$ ms^{-1}, and $\gamma^{-1} = 0-80$ ps. For the fitting, v is taken from the literature[22] and q is determined from the TG signal of azobenzene/ethanol, which is known to relax very rapidly and provide an impulsive response curve.[23] Because of the long period of the oscillation (~500 ps), the uncertainty of the heat-releasing rate is rather large (±40 ps).

As the temperature is decreased, the acoustic signal becomes weaker because of the decrease of $\partial\rho/\partial T$ of water. At the same time, the nonoscillating component becomes apparent. This nonoscillating component can be explained by either the Temp.G or the population grating components. (The signal cannot be due to the optical Kerr signal, which should respond very quickly to the pumping laser pulse (electronic response) or relax very rapidly in nonviscous solution (nuclear response)). The temporal profile of the Temp.G signal, which originated from the first term of eq 1, can be calculated from thermodynamic equations (a typical example is presented in ref 6). Since the acoustic effect in the Temp.G signal of an aqueous solution is very small due to the relation of $C_p/C_v \sim 1$, the signal resembles a step function for a sufficiently fast heating process. When the heat-releasing process is represented by a multiexponential function, $\Sigma\exp(-\gamma_i t)$, the Temp.G signal can be approximated as

$$\Delta n_T(t) \simeq \left(\frac{\partial n}{\partial T}\right)_\rho \sum_i \frac{2Q_i}{\rho_0 C_p}[1 - \exp(-\gamma_i t)] \quad (5)$$

The other possibility, the population grating, is caused by the refractive index change induced by the photoexcited species or photochemical products, which should possess different polarizabilities from that of the original (ground-state) species. The TG signal by this component can be expressed by

$$\Delta n_p = \sum_i R_i C_i(t) \quad (6)$$

TABLE 1: Ratio of the Components of the Dens.G Signal and the Temp.G Signal

temp, °C	n_ρ^0/n_T^0
22	9 ± 4
6	0.25
4	~0
2	−0.42

where R_i is a constant which is determined by the refractive index change by the presence of the transient species and $C_i(t)$ is the concentration of the transient species.

Although it is generally rather difficult to distinguish these components in the TG signal, we attribute the nonoscillating component in this case to the Temp.G signal based on the following three reasons. First, the rise profile of the nonoscillating signal should be fitted with a lifetime of 55 ps as shown later. This temporal delay after the photoexcitation excludes the possibility of the population grating signal which comes from an intermediate species directly excited from the ground state. Second, $FeCl_3$ is frequently used as a calorimetric standard, which shows that all of the photon energy absorbed by this compound is released as heat and no photochemical reaction occurs.[16] Therefore, it is very unlikely that the photochemical intermediates or excited states contribute to the signal for long times (4 ns). Third, the temporal profile of the observed TG signal can be fitted by a superposition of the acoustic signal (eq 3) and a step-functional signal as shown in Figure 1, and we found that the signal intensity of this nonoscillating component is almost what we expect of the Temp.G signal as shown below.

The observed TG signals can be fitted well by the function

$$I_{TG} \simeq (\Delta n_\rho + \Delta n_T)^2 \quad (7)$$

in a wide temperature range (22−2 °C). The intensity ratio of the Temp.G signals is determined by thermodynamic parameters, which are characteristic of the medium,

$$n_\rho^0/n_T^0 = \left(\frac{\partial n}{\partial \rho}\right)_T \left(\frac{\partial \rho}{\partial T}\right)_\rho \Big/ \left(\frac{\partial n}{\partial T}\right)_\rho \quad (8)$$

For calculating these parameters from the observed TG signal, the finite relaxation rate should be taken into consideration in this fast time scale. The ratios of the Temp.G to the Dens.G components (n_ρ^0/n_T^0) thus determined at different temperatures are shown in Table 1. These values agree well with those obtained with the nanosecond laser system previously.[6,7]

3-2. Dynamics of the Photoexcited States of $FeCl_3$. Next, the dynamics of photoexcited $FeCl_3/H_2O$ is discussed based on the TG signal. The rise part of the Temp.G signal is expanded in time and shown in Figure 2. The rise part of this signal is fitted by assuming a single-exponential rise time and by taking into account the finite pulse width, which is measured by the population grating signal from malachite green/ethanol. The solid line shows the calculated signal with $\gamma_i^{-1} = 55(\pm 5)$ ps.

The absorption spectrum of $FeCl_3/H_2O$ (0.2 mM) is shown in Figure 3. It is well-known that iron makes various complexes in aqueous solution. Complexes with chloride ion ($FeCl^{2+}$ or $FeCl_2^+$, etc) can be neglected in such a dilute solution used here.[24,25] From the shape of the spectrum and the value of the absorption coefficient (ϵ), the excited species is identified as $[Fe(OH)(H_2O)_5]^{2+}$.[24,26] The electron configuration of the ferric ion is d^5, and $[Fe(OH)(H_2O)_5]^{2+}$ is a high-spin complex. While the d−d transition is forbidden, the complex ion has several charge-transfer bands in the near-UV region with strong low-

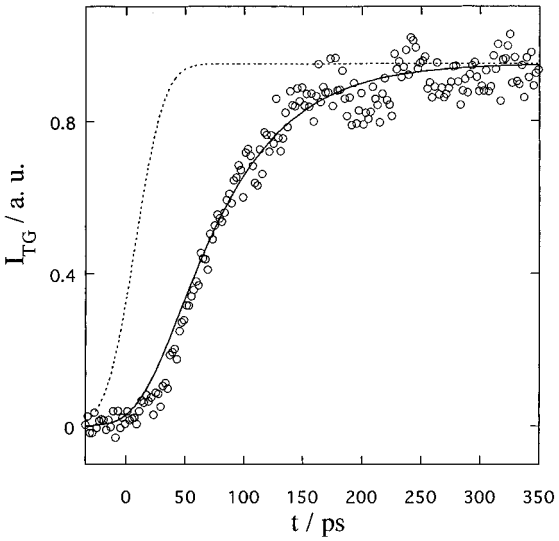

Figure 2. Rise profile of the Temp.G signal of $FeCl_3/H_2O$ (10 mM) at 4 °C. The solid and dotted lines denote the calculated signals with rise times of 55 and 0.1 ps, respectively.

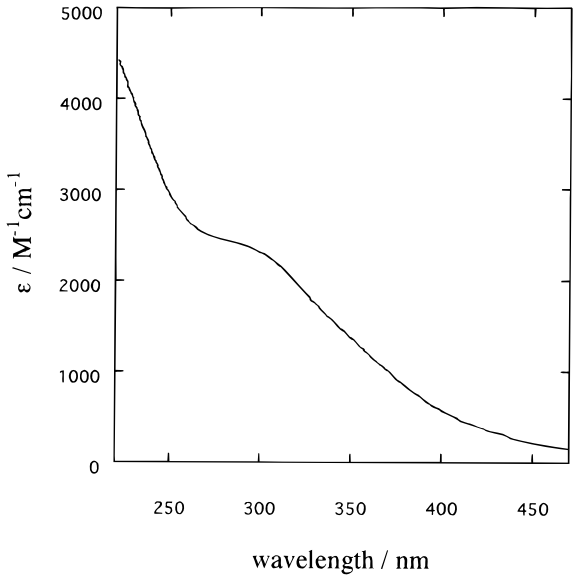

Figure 3. Absorption spectrum of $FeCl_3/H_2O$ (0.2 mM).

energy wings in the visible region.[27] The 355-nm excitation wavelength corresponds to a wing of this charge-transfer band.

There are two possibilities for the interpretation of the 55-ps rising component. First, the temperature rise could represent the relaxation process of the electronically excited state. In this case, since the broad feature of the absorption spectrum should be due to a random distribution of the solvent molecules (water) around the ion (inhomogeneous broadening), it is highly probable that the excited ion first relaxes to the lowest excited state (most stable configuration) very rapidly (within a few picoseconds) and then decays back to the ground state rather slowly with a lifetime of 55 ps. The orientation of water should, then, readjust back to the original configuration. The reorganization time of water can be less than a few picoseconds.[28]

Based on this consideration, it is expected that the observed Temp.G signal should rise with two time constants, the faster one which represents the reorganization time of water and the slower one which represents the rate of the transition between different electronic states. If we assume that the faster rate constant is of the order of 10^{12} s^{-1}, it is found by the fitting of the temporal profile of the Temp.G signal that the intensity for the faster rise should be less than 10% total, which means that

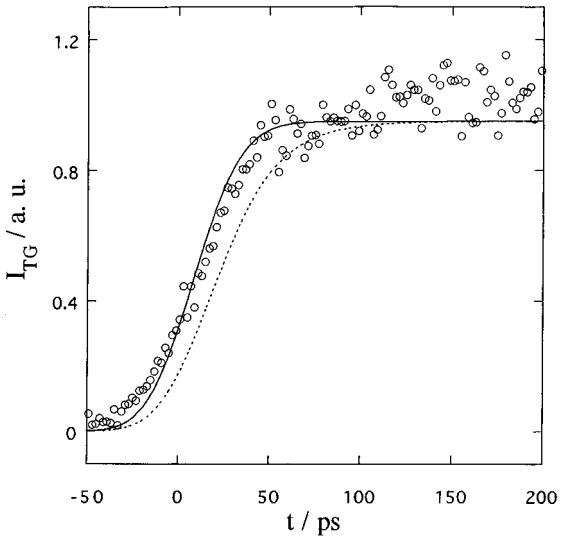

Figure 4. Rise profile of the Temp.G signal of *o*-HBP (0.8 mM)/ SDS/H_2O at 4 °C. The solid line denotes the calculated signal with two rise times of 400 fs and 7.5 ps, and the ratio of their contributions is 1:10. For comparison, the calculated signal with two time constants of 400 fs and 20 ps with an intensity ratio of 1:10 is showed (dotted line).

the reorganization energy should be smaller than ~2600 cm^{-1}. In other words, the photoexcited ferric ion relaxes to the lowest excited level, which should be located in the 350−390 nm range, with a very fast rate and then relaxes to the ground state with the 55-ps lifetime.

The other explanation of the temperature rise is related to the vibrational relaxation in the ground state. The excited electronic state of $[Fe(OH)(H_2O)_5]^{2+}$ could relax in a ultrafast time scale, the energy is transferred to the vibrational freedom of the complex, and then the energy is released to the matrix with a 55-ps time constant.

The above two mechanisms (relaxation between the electronic states or among the vibrational manifold in the ground state) can be tested by a ground-state recovery measurement. Although we have performed this type experiment at 335 nm, any trace of bleach signal was not observed probably because of the small extinction coefficient and the weak laser power. Therefore, at this moment, we cannot conclude which mechanism is proper to describe the energetic dynamics after the photoexcitation of Fe^{3+} in water. However, considering the ultrafast temperature rise (≤3 ps) after the photoexcitation of Ni^{2+} in water,[15] we think that the vibrational relaxation of the solvated water could be very fast. Indeed, this expectation is supported by the molecular dynamics calculation, which indicates that the energy dissipation to the translational manifold is very fast in water within the order of a picosecond.[29] Therefore, at this moment, we think that the first mechanism, the lifetime of the electronic excited state is 55 ps, is plausible.

3-3. Dynamics of the Excited State of *o*-HBP. Using the same temperature variation method, we investigated the photophysical dynamics of the *o*-HBP (0.8 mM)/SDS (25 mM)/ H_2O solution. (SDS is necessary to dissolve *o*-HBP in water.) A similar temperature dependence of the TG signal as the previous one (Figure 1) is observed from this sample (below 4 °C, the TG signal could not be detected because of the precipitation of SDS). The signal can be fitted by a superposition of the acoustic signal and a step-functional-type signal. Following similar arguments as in the previous section, the nonoscillating signal is assigned to the Temp.G signal. At 4 °C, the signal consists of only the Temp.G signal (Figure 4). If

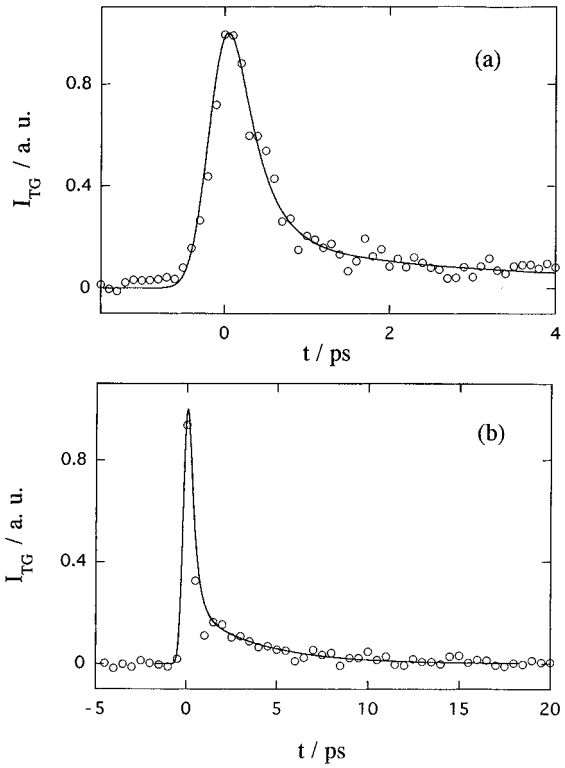

Figure 5. Population grating signals of *o*-HBP/hexane (20 mM). The solid lines denote the biexponential function with lifetimes of 400 fs and 7.5 ps.

we assume that the rise profile can be fitted by a single-exponential function, it gives 6 ± 3 ps rise time.

In order to clarify the photophysical dynamics in more detail, we measured the TG signal of *o*-HBP/hexane (20 mM) using the subpicosecond laser system. (Since the total laser power per pulse of this system is rather weaker than that of the picosecond laser and also the concentration of *o*-HBP cannot be larger in an aqueous solution because of the low solubility, we could not observe the Temp.G and the Dens.G signals from the aqueous solution. It should be noted that the peak power of the picosecond YAG laser is weaker than that of this subpicosecond laser system. Hence, the multiphoton process for the aqueous sample should be negligible.) Upon photoexcitation of this sample by the shorter pulsed laser, a weak population grating signal is observed before the rather strong acoustic signal appears (Figure 5). By taking into account the response function of our system, which is measured by the optical Kerr grating signal from a CCl_4 solution, the temporal profile can be fitted with a biexponential function. The lifetimes of the longer and shorter components are 7.5 ± 1.5 ps and 400 ± 100 fs.

As stated in the Introduction, *o*-HBP is well-known as a photochemical stabilizer and the dynamics of the photoexcited states have been investigated. Photoreduction, intersystem crossing to the T_1 state, and luminescent process upon photoexcitation are very minor processes in solution at room temperature.[17−19] In hexane, which is a non-hydrogen-bonding solvent, only a short-lived component was observed with a lifetime of ∼35 ps, and this component was attributed to the S_1 state of an intramolecularly hydrogen-bonded species.[17] On the other hand, in ethanol, signals of the short-lived (∼30-ps) S_1 state of the intramolecularly hydrogen bonded species and long-lived (∼1.5-ns) T_1 state of the intermolecularly hydrogen bonded species were observed.[17] In the present measurement, any long-lived species which had a lifetime of nanosecond order was not observed. Therefore, only intramolecularly hydrogen-bonded species exist in the SDS/H_2O system. While a 35-ps lifetime for the S_1 state in hexane was obtained by Hou et al., Topp reported a 6 ± 3 ps lifetime.[20] Since our observed lifetime (7.5 ps in hexane) is close to the S_1 lifetime measured by Topp and the signals reported by Hou et al. have large uncertainties, we consider that the lifetime of the S_1 state of *o*-HBP in hexane is 7.5 ps. This value is also close to the lifetime (∼10 ps) in methylene chloride reported by Merritt et al.[18] The faster dynamics (400 fs) observed in the TG signal is attributed to the lifetime of the Franck−Condon state, which is produced directly from the ground state of *o*-HBP. The lifetime may represent the intramolecular vibrational relaxation rate in the S_1 manifold.

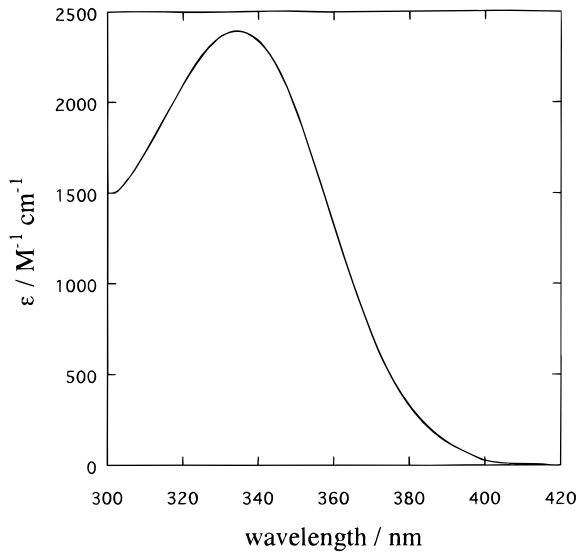

Figure 6. Absorption spectrum of 2-HBP (0.3 mM)/SDS/H_2O.

Considering these dynamics, we reevaluate the observed rise part of the Temp.G signal. The rise of the temperature should be caused by these dynamics. The absorption spectrum of *o*-HBP/SDS/H_2O (0.3 mM) is shown in Figure 6. From this spectrum, the origin of the S_1 state of *o*-HBP is found to be ∼25 600 cm^{-1}. Therefore, we assume that the released energy from the vibrational relaxation in the S_1 state (28 200 cm^{-1}− 25 600 cm^{-1} = 2600 cm^{-1}) should appear with a time constant of 400 fs and then the energy released by the $S_1 \rightarrow S_0$ internal conversion appears with a lifetime of 7.5 ps.

The solid line in Figure 4 is the calculated temperature increase based on the mechanism described above. This calculated curve reproduces the observed signal. (As long as the intensity ratio is 1:10, the faster deactivation rate is not an important parameter for the fitting. For example, the lifetime of the weaker component can be 0−9 ps for a reasonable fitting.) If we freely adjust the lifetime of the main component as a parameter for the fitting, the observed signal can be reproduced with 5−12 ps within our experimental uncertainty. If we assume that the temperature of the solution rises with a finite time constant after deactivation of the S_1 state, the time constant of the Temp.G rise should be given by a convolution of the S_1 lifetime and the thermalization time constant. However, the upper limit of the rise time is 12 ps, which is close to the observed lifetime of the S_1 state (7.5 ± 1.5 ps). Therefore, we must conclude that the thermalization process, which could be determined by the vibrational relaxation in the ground state, should be faster than ∼5 ps. Recently, Terazima found that the thermalization process after the photoexcitation of Ni^{2+} in aqueous solution is also very fast (less than 3 ps).[15] The above observation is consist with this result.

4. Conclusion

In this paper, it is demonstrated that the new TG (Temp.G) signal has a few picoseconds of time resolution. From the rise part of the Temp.G signal after the photoexcitation of $FeCl_3$/H_2O, the lifetime of the main relaxation process is found to be about 55 ps. The Temp.G signal after the photoexcitation of *o*-HBP/SDS/H_2O rises much faster than 35 ps, which was reported as the lifetime of the S_1 state in hexane. From the temporal profile of the population grating signal of *o*-HBP/hexane, we observed two time constants for the dynamics of the excited states, 400($\pm$100) fs and 7.5($\pm$1.5) ps. The shorter component is attributed to the vibrational relaxation in the S_1 manifold, and the longer one is assigned to the lifetime of the S_1 state of intramolecularly hydrogen-bonded species. The rise profile of the Temp.G signal can be fitted by using these values, and the estimated energy level of the S_1 state is $\sim$25 600 cm^{-1}. Since this method (Temp.G together with the Temp.L method) is the only technique which can detect the thermal energy in a very fast time scale, it will be useful for studying various fast energetic dynamics.

References and Notes

(1) Andrews, J. R.; Hochstrasser, R. M. *Chem. Phys. Lett*. **1980**, *76*, 207.
(2) Fayer, M. D. *Annu. Rev. Phys. Chem*. **1982**, *33*, 63.
(3) Genberg, L.; Bao, Q.; Gracewski, S.; Miller, J. D. *Chem. Phys.* **1989**, *131*, 81.
(4) Zimmt, M. B. *Chem. Phys. Lett.* **1989**, *160*, 564.
(5) Morais, J.; Ma, J.; Zimmt, M. B. *J. Phys.Chem*. **1991**, *95*, 3885.
(6) Terazima, M. *Chem. Phys*. **1994**, *189*, 793.
(7) Terazima, M. *J. Chem. Phys*. **1996**, *104*, 4988.
(8) Takezaki, M.; Hirota, N.; Terazima, M. *J. Phys. Chem*. **1996**, *100*, 10015.
(9) Scarlet, R. I. *Phys. Rev.* **1972**, *6*, 2281.
(10) Desai, R. C.; Levenson, M. D.; Barker, J. A. *Phys. Rev*. **1983**, *A27*, 1968.
(11) Elsaesser, T.; Kaiser, W. *Annu. Rev. Phys. Chem*. **1991**, *42*, 83.
(12) Ashworth, S. H.; Hasche, T.; Woerner, M.; Riedle, E.; Elsaesser, T. *J. Chem. Phys.* **1996**, *104*, 5761.
(13) Terazima, M.; Hirota, N. *J. Chem. Phys.* **1994**, *100*, 2481.
(14) Terazima, M. *Chem. Phys. Lett*. **1994**, *230*, 87.
(15) Terazima, M. *J. Chem. Phys.* **1996**, *105*, 6587.
(16) Braslavsky, S. E.; Heibel, G. E. *Chem. Rev*. **1992**, *92*, 1381.
(17) Hou, S. Y.; Hetherington, W. M., III; Korenowski, G. M.; Eisenthal, K. B. *Chem. Phys. Lett*. **1979**, *68*, 282.
(18) Merritt, C.; Scott, G. W.; Gupta, A.; Yavrouian, A. *Chem. Phys. Lett.* **1980**, *69*, 169.
(19) Scaiano, J. C. *Chem. Phys. Lett.* **1982**, *92*, 97.
(20) Topp, M. R. Unpublished results cited in ref 18.
(21) Eichler, H. J.; Günter, P.; Pohl, D. W. *Laser-Induced Dynamic Gratings*; Springer-Verlag: Berlin, 1986.
(22) Hall, L. *Phys. Rev*. **1948**, *73*, 775.
(23) (a) Struve, W. S. *Chem. Phys. Lett*. **1977**, *46*, 15. (b) Morgante, C. G.; Struve, W. S. *Chem. Phys. Lett*. **1979**, *68*, 267.
(24) Rabinowitch, E.; Stockmayer, W. H. *J. Am. Chem. Soc*. **1942**, *64*, 335.
(25) Gamlen, G. A.; Jordan, D. O. *J. Chem. Soc*. **1953**, 1435.
(26) Rabinowitch, E. *Rev. Mod. Phys.* **1942**, *14*, 112.
(27) Cotton, F. A.; Wilkinson, G. *Advanced Inorganic Chemistry*, 5th ed.; John Wiley & Sons: New York, 1988.
(28) (a) Chang, Y. J.; Castner, E. W., Jr. *J. Chem. Phys.* **1993**, *99*, 113. (b) Palese, S.; Schilling, L.; Miller, R. J. D.; Staver, P. R.; Lotshaw, W. T. *J. Phys. Chem.* **1994**, *98*, 6308.
(29) Ohmine, I. *J. Chem. Phys.* **1986**, *85*, 3342.